
Machine Learning Assisted Bayesian Calibration of Model Physics Parameters for Wetland Methane Emissions: A Case Study at a FLUXNET-CH₄ Site

Sandeep Chinta¹, Xiang Gao¹, Qing Zhu²

¹Center for Global Change Science, Massachusetts Institute of Technology, Cambridge, Massachusetts, USA.

²Climate and Ecosystem Sciences Division, Climate Sciences Department, Lawrence Berkeley National Laboratory, Berkeley, California, USA.

sandeepc@mit.edu, xgao304@mit.edu, qzhu@lbl.gov

Abstract

1 Methane (CH₄) possesses a notably higher warming potential than carbon dioxide
2 despite its lower atmospheric concentration, making it integral to global climate
3 dynamics. Wetlands stand out as the predominant natural contributor to global
4 methane emissions. Accurate modeling of methane emissions from wetlands is
5 crucial for understanding and predicting climate change dynamics. However, such
6 modeling efforts are often constrained by the inherent uncertainties in model
7 parameters. Our work leverages machine learning (ML) to calibrate five physical
8 parameters of the Energy Exascale Earth System Model (E3SM) land model
9 (ELM) to improve the model’s accuracy in simulating wetland methane
10 emissions. Unlike traditional deterministic calibration methods that target a single
11 set of optimal values for each parameter, Bayesian calibration takes a probabilistic
12 approach and enables capturing the inherent uncertainties in complex systems and
13 providing robust parameter distributions for reliable predictions. However,
14 Bayesian calibration requires numerous model runs and makes it computationally
15 expensive. We employed an ML algorithm, Gaussian process regression (GPR),
16 to emulate the ELM’s methane model, which dramatically reduced the
17 computational time from 6 CPU hours to just 0.72 milliseconds per simulation.
18 We exemplified the procedure at a representative FLUXNET-CH₄ site (US-PFa)
19 with the longest continuous methane emission data. Results showed that the
20 default values for two of the five parameters examined were not aligned well with
21 their respective posterior distributions, suggesting that the model’s default
22 parameter values might not always be optimal for all sites, and that site-specific
23 analysis is warranted. In particular, analyses at sites with different vegetation
24 types and wetland characteristics could reveal more useful insights for
25 understanding methane emissions modeling.

26 1 Introduction and Motivation

27 Greenhouse gas (GHG)-induced climate change poses unprecedented challenges and serious risks
28 for human society and natural environment. Methane is the second most important GHG, with ~25
29 times stronger 100-year global warming potential than carbon dioxide [1, 2]. Since the Industrial
30 Revolution, the atmospheric concentrations of CH₄ have sharply risen and doubled since pre-
31 industrial times. Alarmingly, its growth rate in 2021 marked the highest record since 1984 [3–5].
32 Such increases have profound implications for global warming and highlight the urgency to manage
33 its emissions effectively. Wetlands account for approximately 30% of global methane emissions and
34 are the primary natural source [6]. However, wetland methane emission estimates based on
35 biogeochemistry models remain highly uncertain [7, 8], mainly because CH₄ dynamics rely on a
36 large number of poorly constrained model parameters to characterize a diverse array of physical,

37 biological, and chemical processes [9, 10]. While these parameters typically have fixed (default)
38 values, their exact values are often ambiguous and present large uncertainty. The parameter values
39 are usually determined within their theoretically plausible uncertainty ranges based on the most
40 reliable knowledge available. One of the essential paths to achieve reduced biases in methane
41 emission estimates is to identify the most critical model parameters via sensitivity analysis and
42 determine their optimal distribution through calibration.

43 Traditional deterministic calibration methods focus on identifying an optimal parameter value by
44 comparing model output to observations, frequently neglecting the inherent predictive uncertainties
45 and incorrectly assuming that there is always a single set of optimal values for all parameters [11].
46 Nevertheless, a single optimal set may not always exist for a problem. Even if it exists, the associated
47 uncertainties could be large. Moreover, several alternative parameter configurations may yield
48 similarly accurate results, challenging the notion of a single optimal parameter set [12, 13].
49 Considering these challenges posed by the deterministic calibration methods and the inherent
50 complexities of methane models, there is a need for a more nuanced and statistically rigorous
51 approach to parameter calibration. Probabilistic approaches like Bayesian calibration handle these
52 issues by statistically representing parameter uncertainties [14]. The input parameter space is
53 represented as probability distributions of parameters. Multiple parameter samples are drawn from
54 this distribution, and simulations are conducted for these samples, inherently creating an ensemble
55 of model predictions. An objective function is used to evaluate the prediction range by comparing
56 these simulation outputs with observations. After calibration, final posterior distributions of the
57 parameters are obtained. When samples are drawn from these distributions, the resulting
58 simulations, forming an ensemble, more closely match the observations. However, it is important
59 to note that this approach generally requires massive computational power to simulate the methane
60 model multiple times. Hence, there is a compelling need for strategies like machine learning that
61 can facilitate this process but also retain accuracy. ML-based emulators have emerged as a pivotal
62 tool to emulate the behavior of complex earth system models for achieving this goal. These
63 emulators are first trained on a subset of model simulations to learn the intricate relationships
64 between inputs and outputs. The trained emulators can then be used to predict the model's response
65 for a new set of parameters, effectively eliminating the need for exhaustive simulations every time
66 there is a change in parameter values. This approach is particularly advantageous for Bayesian
67 calibration, where thousands of simulations are needed to explore the parameter uncertain space
68 adequately. Until now the attempt is still very few for applying this probabilistic approach to predict
69 wetland methane emissions from land models.

70 This study aims to bridge the gap between the intensive computational demands of Bayesian
71 calibration and the desired accuracy in wetland methane emission modeling. This is achieved by
72 emulating the ELM with the Gaussian Process Regression (GPR) ML algorithm. We leverage
73 observed CH₄ emission data from a specific FLUXNET-CH₄ site (US-PFa) as a case study. We
74 select five model parameters and train GPR for estimating the error associated with methane
75 emission outputs. Our primary objective is to minimize the error between the emulator-estimate
76 emissions and corresponding observations. While we only focus on one site, the demonstrated
77 methodology is expected to be easily extended to other FLUXNET-CH₄ sites with much broader
78 applicability.

79 **2 Model parameters and FLUXNET-CH₄ site (US-PFa) data**

80 We configured the most recent version of the Energy Exascale Earth System Model (E3SM) land
81 model (ELM) (<https://github.com/E3SM-Project/E3SM>), which contains many added new features
82 for the CH₄ dynamics modeling [15]. In previous studies, a comprehensive sensitivity analysis was
83 conducted for 19 ELM parameters associated with different CH₄ dynamic processes and five
84 parameters are identified as sensitive for methane emission [16]. These five sensitive parameters are
85 presented in Table 1 along with their default values, theoretical ranges, and brief description. A
86 uniform prior distribution is assumed for these parameters. Our objective is to identify a posterior
87 distribution of these five parameters to minimize the emission prediction error.

88 FLUXNET-CH₄ is a global network of sites that provides continuous, high-frequency, and quality-
89 checked CH₄ emission flux measurements. US-PFa [17]([https://ameriflux.lbl.gov/sites/siteinfo/US-
90 PFa](https://ameriflux.lbl.gov/sites/siteinfo/US-PFa)) with longest continuous available data is chosen for our study. The monthly averaged data

91 from this site is used to evaluate the monthly averaged site-specific simulated emissions from ELM
 92 model for various parameter samples.

93 Table 1: List of 5 ELM parameters used and their default values, ranges, and brief description.

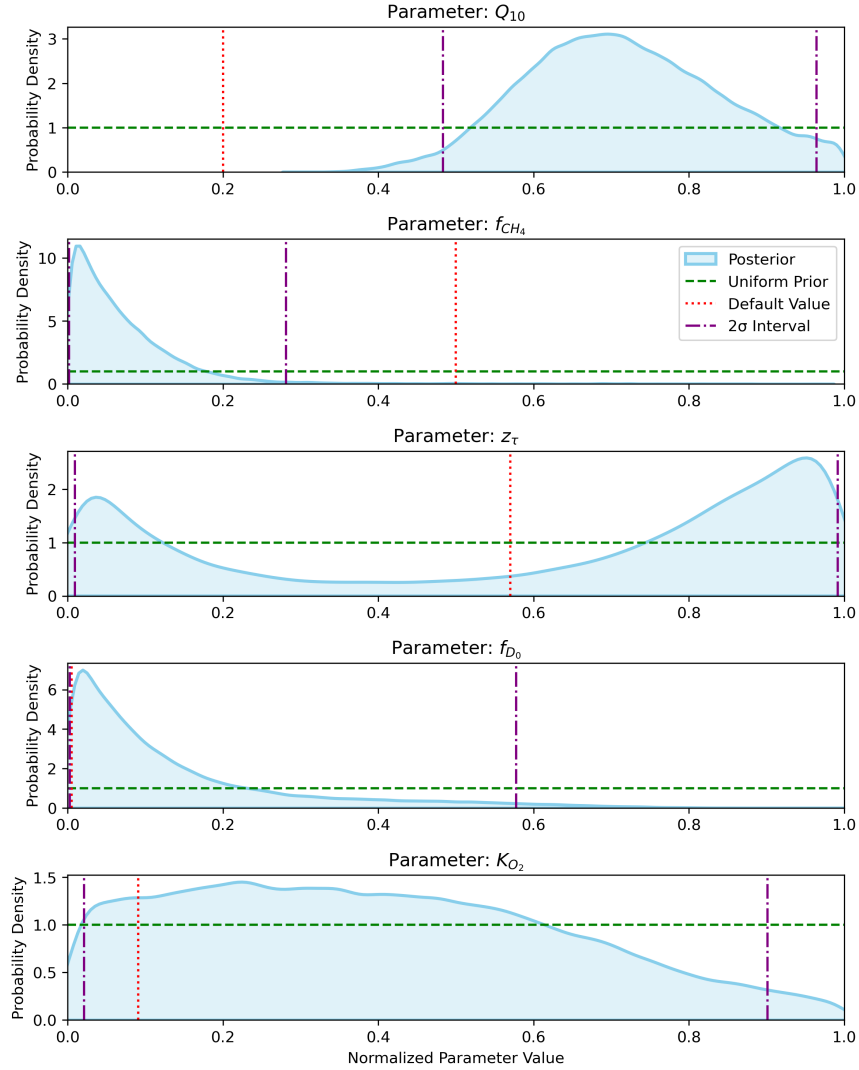
Mechanism	Parameter	Default	Range	Units	Description
Production	Q_{10}	2	[1.5 4]	-	CH ₄ production Q_{10}
	f_{CH_4}	0.2	[0.1 0.3]	-	Ratio between CH ₄ and CO ₂ production below the water table
Substrate availability	z_τ	0.5	[0.1 0.8]	m	e-folding depth for decomposition
Diffusion	f_{D_o}	1	[1 10]	m ² s ⁻¹	Diffusion coefficient multiplier
Oxidation	K_{O_2}	2×10^{-2}	$\left[\frac{2 \times 10^{-3}}{2 \times 10^{-1}} \right]$	mol m ⁻³	O ₂ half-saturation oxidation coefficient

94 3 Methodology and Results

95 A commonly adhered guideline [18] suggests using a sample size ten times the number of model
 96 parameters for training ML models. Following this, we generated sixty samples (exceeding the 10*5
 97 criterion) of diverse parameter values using Latin Hypercube Sampling (LHS) [19] to train the GPR.
 98 Another set of 20 independent LHS samples are generated to test the GPR fit. Simulations are also
 99 conducted with the ELM methane model based on these 80 samples and the corresponding root-
 100 mean-square-error (RMSE) for each simulation is evaluated using observed monthly averaged
 101 emissions. The RMSE values from these 80 simulations is normalized by dividing with RMSE value
 102 from the simulation with default parameter values. This is referred to as normalized RMSE
 103 (nRMSE). Any value of nRMSE < 1 implies that the parameter sample is better than default. Ideally,
 104 we would want nRMSE closer to 0. GPR is trained with normalized parameter values in the ranges
 105 from Table 1 (normalized to [0 1] using MinMax scaling) as inputs and nRMSE values as outputs
 106 with the 60 simulations. Subsequent testing of the trained GPR on 20 test samples results in an R^2
 107 value of 0.92, indicating a strong model fit. This GPR model is subsequently employed for Bayesian
 108 calibration.

109 Bayesian calibration is a process of updating our beliefs about model parameters based on observed
 110 data. We start with prior beliefs (priors), minimize nRMSE (likelihood), and then update our beliefs
 111 to obtain the posterior distribution. Markov Chain Monte Carlo (MCMC) [20] is employed (using
 112 ‘emcee’ package [21], which is particularly efficient for multi-dimensional problems) to construct
 113 a Markov chain where the stationary distribution (the distribution to which the chain converges over
 114 time) is the desired posterior distribution. By running the chain for a sufficient number of steps
 115 (12000) and discarding an initial set of “burn-in” samples (3000), we obtain samples that
 116 approximate the posterior distribution. Convergence of the MCMC chains is ensured by
 117 implementing the Gelman-Rubin diagnostic (\hat{R}) to check for convergence [22, 23]. A value of \hat{R}
 118 close to 1 for all parameters indicate convergence. $\hat{R}_{1,2,3,4,5} = (1.022, 1.032, 1.042, 1.011, 1.019)$.
 119 This implies that the parameters converged to a posterior distribution minimizing the nRMSE and
 120 the distributions are presented in Figure 1. The mean nRMSE of the posterior distribution of
 121 parameters is 0.228, which is a remarkable 77.2% reduction in error compared to default. The 2σ
 122 range (95% confidence) of nRMSE is [0.199 0.254], which depicts a significant improvement from
 123 default.

124 The posterior distribution of parameters in Fig. 1 offers several insights. The default parameter
 125 values for Q_{10} and f_{CH_4} are outside the 2σ interval, which indicates these parameters likely have true
 126 values different from the default values. Even though z_τ has its default value within the 2σ interval,
 127 it is less likely than the values near the bounds (a bi-modal distribution). The posterior distribution
 128 of K_{O_2} is closer to uniform distribution, which is our prior distribution, implying that this
 129 parameter is not very sensitive to methane emission at US-PFa site.



130

131 Fig. 1: Posterior distribution of five parameters following Bayesian calibration, plotted over a
 132 normalized parameter range. The red vertical line denotes the default value of the parameter. The
 133 green horizontal line denotes the prior distribution, which was the uniform distribution. The 2σ
 134 interval, encompassing 95% of the distribution's values, is marked by violet vertical lines.

135 4 Conclusions and Future Work

136 Our study delves into the crucial challenge of accurately predicting wetland methane emissions by
 137 adjusting ELM parameters using Bayesian calibration. Employing a machine learning algorithm
 138 (GPR) as an emulator for the ELM demonstrates significant potential in reducing computational
 139 demand. A remarkable improvement of 77% (normalized RMSE) was achieved compared to the
 140 default model parameters. This deviation of posterior distributions from the default values highlights
 141 that models may require fine-tuning to address site-specific nuances, particularly when addressing
 142 heterogeneous systems like wetlands. While our study focused on the US-PFa FLUXNET-CH₄ site,
 143 the presented methodology is universally applicable. This methodology can be easily extended to
 144 global wetland ecosystems with different vegetation types to get further insights into wetland
 145 methane emissions dynamics and relevant parameters. As methane emissions have seasonal
 146 fluctuations, it is our future interest to explore whether the posterior distributions change relative to
 147 seasons.

148
149
150
151
152
153
154
155
156
157
158
159
160
161
162
163
164
165
166
167
168
169
170
171
172
173
174
175
176
177
178
179
180
181
182
183
184
185
186
187
188
189
190
191
192
193
194
195
196
197
198
199
200
201
202
203
204
205
206

References

1. Solomon, S., others: Climate change 2007: the physical science basis. Contribution of Working Group I to the Fourth Assessment Report of the Intergovernmental Panel on Climate Change. 4, (2007)
2. IPCC: Climate Change 2013: The Physical Science Basis. Contribution of Working Group I to the Fifth Assessment Report of the Intergovernmental Panel on Climate Change. Presented at the (2013)
3. Saunio, M., Stavert, A.R., Poulter, B., Bousquet, P., Canadell, J.G., Jackson, R.B., Raymond, P.A., Dlugokencky, E.J., Houweling, S., Patra, P.K., others: The Global Methane Budget 2000–2017. *Earth Syst Sci Data*. 12, 1561–1623 (2020)
4. Lan, X., Thoning, K.W., Dlugokencky, E.J.: Trends in globally-averaged CH₄, N₂O, and SF₆ determined from NOAA Global Monitoring Laboratory measurements, (2023)
5. Dlugokencky, E.J., Bruhwiler, L., White, J.W.C., Emmons, L.K., Novelli, P.C., Montzka, S.A., Masarie, K.A., Lang, P.M., Crotwell, A.M., Miller, J.B., others: Observational constraints on recent increases in the atmospheric CH₄ burden. *Geophys Res Lett*. 36, (2009)
6. Kirschke, S., Bousquet, P., Ciais, P., Saunio, M., Canadell, J.G., Dlugokencky, E.J., Bergamaschi, P., Bergmann, D., Blake, D.R., Bruhwiler, L., others: Three decades of global methane sources and sinks. *Nat Geosci*. 6, 813–823 (2013)
7. Jackson, R.B., Saunio, M., Bousquet, P., Canadell, J.G., Poulter, B., Stavert, A.R., Bergamaschi, P., Niwa, Y., Segers, A., Tsuruta, A.: Increasing anthropogenic methane emissions arise equally from agricultural and fossil fuel sources. *Environmental Research Letters*. 15, 71002 (2020)
8. Rosentreter, J.A., Borges, A. V., Deemer, B.R., Holgerson, M.A., Liu, S., Song, C., Melack, J., Raymond, P.A., Duarte, C.M., Allen, G.H., others: Half of global methane emissions come from highly variable aquatic ecosystem sources. *Nat Geosci*. 14, 225–230 (2021)
9. Riley, W.J., Subin, Z.M., Lawrence, D.M., Swenson, S.C., Torn, M.S., Meng, L., Mahowald, N.M., Hess, P.: Barriers to predicting changes in global terrestrial methane fluxes: analyses using CLM4Me, a methane biogeochemistry model integrated in CESM. *Biogeosciences*. 8, 1925–1953 (2011)
10. Ricciuto, D.M., Xu, X., Shi, X., Wang, Y., Song, X., Schadt, C.W., Griffiths, N.A., Mao, J., Warren, J.M., Thornton, P.E., others: An integrative model for soil biogeochemistry and methane processes: I. Model structure and sensitivity analysis. *J Geophys Res Biogeosci*. 126, e2019JG005468 (2021)
11. Hoversten, G.M., Cassassuce, F., Gasperikova, E., Newman, G.A., Chen, J., Rubin, Y., Hou, Z., Vasco, D.: Direct reservoir parameter estimation using joint inversion of marine seismic AVA and CSEM data. *Geophysics*. 71, C1–C13 (2006)
12. Gupta, H.V., Sorooshian, S., Yapo, P.O.: Toward improved calibration of hydrologic models: Multiple and noncommensurable measures of information. *Water Resour Res*. 34, 751–763 (1998)
13. Van Straten, G.T., Keesman, K.J.: Uncertainty propagation and speculation in projective forecasts of environmental change: A lake-eutrophication example. *J Forecast*. 10, 163–190 (1991)
14. Beven, K., Binley, A.: The future of distributed models: model calibration and uncertainty prediction. *Hydrol Process*. 6, 279–298 (1992)
15. Zhu, Q., Riley, W.J., Tang, J., Collier, N., Hoffman, F.M., Yang, X., Bisht, G.: Representing nitrogen, phosphorus, and carbon interactions in the E3SM land model: Development and global benchmarking. *J Adv Model Earth Syst*. 11, 2238–2258 (2019)
16. Chinta, S., Gao, X., Zhu, Q.: Sensitivity Analysis and Uncertainty Quantification of E3SM Methane model using Machine Learning. In: AGU Fall Meeting Abstracts. pp. B16D-02 (2022)
17. Desai, A.R., Xu, K., Tian, H., Weishampel, P., Thom, J., Baumann, D., Andrews, A.E., Cook, B.D., King, J.Y., Kolka, R.: Landscape-level terrestrial methane flux observed from a very tall tower. *Agric For Meteorol*. 201, 61–75 (2015)
18. Loepky, J.L., Sacks, J., Welch, W.J.: Choosing the sample size of a computer experiment: A practical guide. *Technometrics*. 51, 366–376 (2009)
19. McKay, M.D., Conover, W.J., Beckman, R.J.: A comparison of three methods for selecting values of input variables in the analysis of output from a computer code. *Technometrics*. 21, 239–245 (1979)
20. Brooks, S., Gelman, A., Jones, G., Meng, X.-L.: Handbook of markov chain monte carlo. CRC press (2011)
21. Foreman-Mackey, D., Hogg, D.W., Lang, D., Goodman, J.: emcee: the MCMC hammer. *Publications of the Astronomical Society of the Pacific*. 125, 306 (2013)
22. Gelman, A., Rubin, D.B.: Inference from iterative simulation using multiple sequences. *Statistical science*. 7, 457–472 (1992)
23. Vats, D., Knudson, C.: Revisiting the gelman–rubin diagnostic. *Statistical Science*. 36, 518–529 (2021)